THE EFFECT OF ION IMPLANTATION OF SELECTED DOPANTS ON SOME OF THE ELECTRICAL PROPERTIES OF UO_2

M. Jonathan Haire
Nuclear Science and Technology Division
Oak Ridge National Laboratory*
Oak Ridge, TN 37831-6179
e-mail: hairemj@ornlgov, phone: (865) 574-7141

B. G. von Roedern
National Center for Photovoltaics
National Renewable Energy Laboratory
Golden, CO 80401-3393,
e-mail: bolko_von_roedern@nrel.gov, phone: (303) 384-6480

Thomas T. Meek
Materials Science and Engineering Department
The University of Tennessee
Knoxville, TN 37996
e-mail: tmeek1@utk.edu, phone: (865) 974-0940

J. Tesmer and C. Wetteland
Los Alamos National Laboratory
Los Alamos, NM 87544
e-mail: tesmer@lanl.gov, phone: (505) 667-6133

For the
Waste Management 2003 Symposium
Tucson, Arizona
February 23–27, 2003

The submitted manuscript has been authored by a contractor of the U.S. Government under contract DE-AC05-00OR22725. Accordingly, the U.S. Government retains a nonexclusive, royalty-free license to publish or reproduce the published form of this contribution or allow or allow others to do so, for U.S. Government purposes.

---

*Oak Ridge National Laboratory, managed by UT-Battelle, LLC, for the U.S. Department of Energy under contract DE-AC05-00OR22725.

THE EFFECT OF ION IMPLANTATION OF SELECTED DOPANTS ON SOME OF THE ELECTRICAL PROPERTIES OF UO_2

M. Jonathan Haire
Nuclear Science and Technology Division
Oak Ridge National Laboratory*
Oak Ridge, TN 37831-6179
e-mail: hairemj@ornlgov, phone: (865) 574-7141

B. G. von Roedern
National Renewable Energy Laboratory
Golden, CO 80401-3393
e-mail: bolko_von_roedern@nrel.gov, phone: (303) 384-6480

Thomas T. Meek
Materials Science and Engineering Department
The University of Tennessee
Knoxville, TN 37996
e-mail: tmeek1@utk.edu, phone: (865) 974-0940

J. Tesmer and C. Wetteland
Los Alamos National Laboratory
Los Alamos, NM 87544
e-mail: tesmer@lanl.gov, phone: (505) 667-6133

ABSTRACT

The United States Department of Energy (DOE) has ~1 billion pounds of surplus depleted uranium (i.e., uranium tails) from uranium gaseous diffusion enrichment facilities. Rather than treating this material as waste, DOE is investigating potential beneficial uses for this uranium. Of the many possible uses, uranium dioxide (UO_2) has properties that make it equal to or better than conventional photovoltaic (e.g., solar cell) materials. For example, the electronic bandgap of UO_2 occurs at an efficiency equal to that of GaS and Si, and it has five radiation adsorption peaks instead of one. This paper describes the experimental work being conducted to develop urania photovoltaic devices.

INTRODUCTION

Uranium is used as fuel for nuclear power plants and for weapons. However, little effort has been devoted to establishing other uses. The United States Department of Energy has initiated the Depleted Uranium Uses Research and Development Project to evaluate other potential beneficial uses of uranium (1). As part of the Project's effort to evaluate photovoltaic (e.g., solar cell) applications, single-crystal UO_2 samples were characterized as to their electrical and electro-optical properties. Properties of polycrystalline UO_2 were reported earlier (2, 3, 4). In this study, single-crystal UO_2 samples were ion implanted (i.e., doped) at the Ion Beam Materials Laboratory at Los Alamos National Laboratory (LANL). Implantation depths ranged from a few hundred to a couple of thousand angstroms. Dopant

doses ranged from 10^{11} to 10^{17} atoms/cm^2. Implantation energies ranged from 150 to 300 keV, resulting in a dopant depth ranging from ~10^3 µm to over 3×10^3µm. Data were obtained on depleted uranium dioxide doped with Te, Al, Cl, and Cu. Electrical characterization of doped single-crystal samples is reported as well as activation energies for electronic conduction in the intrinsic (i.e., undoped) material. Also, dark current (I_d) and photocurrent data are reported. Earlier work by Bates (5) reported the intrinsic electrical conductivity of UO_2 to be 1.5×10^{-3} S/cm at room temperature, while work by Killeen (6) reported results obtained by doping with niobium. Earlier work by Meek (2) reported on the effect of various dopants on electrical properties of polycrystalline UO_2.

EXPERIMENTAL

Table I gives deposition parameters for the dopants. Ion implantation of the dopants into UO_2 (both crystalline and polycrystalline) was performed in the Ion Beam Materials Laboratory at LANL. All of the samples characterized and reported on in this paper were single crystals of urania grown by the arc fusion method. After the implantation process, the single-crystal samples were heated for several hours in a vacuum at 350ºC to ensure that the samples were not hyperstoichiometric.

Table I. Deposition Parameters for Single-Crystal UO_2 Samples

Sample no.	Dopant	Energy (keV)	Deposition depth (Å)	Dopant concentration (at/cm^3)	Dose (at/cm^2)
5C	Te	300	528	10^{17}	9.5×10^{11}
4C	Te	300	528	10^{19}	9.5×10^{13}
20C	Te	300	528	10^{21}	9.5×10^{15}
32C	Al	150	1050	10^{17}	2.75×10^{12}
30C	Al	150	1050	10^{19}	2.75×10^{14}
27C	Al	150	1050	10^{21}	2.75×10^{16}
19C	Cl	300	1531	10^{17}	9.59×10^{12}
21C	Cl	300	1531	10^{19}	9.59×10^{14}
22C	Cl	300	1531	10^{21}	9.59×10^{16}
3C	Cu	300	892	10^{21}	1.8×10^{16}

Data for dark and light current were obtained on samples with a constant applied voltage of 5 Vdc. Lastly, temperature-dependent currents were measured over a temperature range of 180 to 450 K, in which the applied voltage varied from 0.5 to 0.732 Vdc. For all electrical measurements, samples were contacted by using spring-loaded probes that were pressed onto silver painted strips ~4 mm long by 2 mm wide separated by a distance of ~2 mm. Illumination intensity in all cases was ~1 sun.

RESULTS AND DISCUSSION

Data for the control sample (an undoped single crystal of UO_2 fabricated using the arc fusion method) are shown in Fig. 1. The peak I_d and peak light current (I_L) values were 15.1 and 57.1 μA, respectively, with an applied voltage of 5 Vdc. When the applied voltage was raised to 10 Vdc, the I_d peak became 26.9 μA and the I_L peak increased to 113.3 μA. The contacts made to the intrinsic material are fairly ohmic because superlinearity (i.e., nonohmic behavior) in current did not depend on the polarity of the applied voltage. Once the light was turned on, it took 1350 s for I_L to reach its peak value (with an applied voltage of 10 Vdc). At the I_L peak, the light was turned off and the current decreased to its initial value in ~1800 s. For the case in which the applied voltage was 5 Vdc, it took ~1080 s to reach the I_L peak and then another 780 s to decay back to its original value of 15 μA. Temperature-dependent current (I_t) data were gathered from ~80 to 450 K. The slope of log(I_t) vs 1000/T defines the activation energy for conduction, and for intrinsic UO_2, this value was found to be 0.26 eV.

There are distinct sample-to-sample differences in the time-dependent behavior of the current. It is difficult to quantitatively define how light affects the magnitude of the current, because some heating occurs as a result of light exposure. Also, small current changes occurred prior to turning on the light. This unusual behavior has now been confirmed for single-crystal UO_2, while our earlier work (3) showed such behavior for polycrystalline samples. Such time-dependent changes in conductivity are not common in material with conductivities as high as those observed for doped and undoped UO_2.

Doping single-crystal UO_2 produced a marked increase in I_L and I_d, with the greatest increase observed for the samples doped with Al, as shown in Fig. 2. At a concentration of 10^{21} atoms of aluminum/cm^3, the observed I_d started at 9.8 mA and increased to 11.6 mA over a 570-s period. At 570 s into the experiment, the light was turned on and the current increased instantaneously to 12.3 mA. Over the next 540 s, the current increased to a peak value of 12.8 mA. When UO_2 was doped to a concentration of 10^{19} atoms of aluminum/cm^3, the peak I_d was 6.3 mA, and the peak I_L became 8.7 mA, after 1590 s of illumination. For a concentration of 10^{17} atoms/cm^3, the peak I_d was 5 mA after 240 s, and the peak I_L as found to be 6.7 mA after 2290 s of illumination.

Figure 3 shows I_d and I_L vs time for UO_2 doped with Te. Table II gives peak I_d, peak I_L, and activation energy for electronic conduction for data for urania doped with Al, Te, Cl, and Cu.

In an earlier paper (2), similar results were reported for polycrystalline UO_2 doped with several of the above solutes. Comparing the earlier work with the work reported here, it is evident that the I_d and I_L values observed for doped single-crystal UO_2 are approximately an order of magnitude greater than those observed in polycrystalline UO_2. The qualitative time dependence for both polycrystalline and single-crystal UO_2 samples is similar.

Figure 4 shows temperature-dependent dark currents (I_t) vs the reciprocal of temperature for Al and Cl. This curve is typical for the doped UO_2 also. The activation energy for conduction of each dopant species was determined from the slope of the respective curve. Activation energies ranged from 0.26 to 0.14 eV in UO_2 doped with Te, Al, and Cl. Higher doping was often correlated with higher currents (conductivity) and lower activation energies. However, in terms of conventional semiconductor doping behavior, the dependencies of the currents on the implanted atomic concentrations are often weak, more like the doping behavior of transparent conductors. Doping with Cu appears relatively ineffective and results in a low current (conductivity) and large activation energy; Al doping leads to high current (conductivities) and lower activation energies even at the low dopant concentration of 10^{17} cm^3. Regardless of the atomic species implanted, use of a thermal probe indicated that all samples were p-type.

Table II. Some Electrical and Electro-Optical Property Data for Intrinsic and Doped UO_2

Sample	Dopant	Dopant concentration (at/cm^3)	Peak I_d (mA)	Peak I_L (mA)	Activation energy for electronic conduction (eV)
16C	Intrinsic UO_2	0	0.0151	0.0571	0.26
5C	Te	10^{17}	3.76	5.76	0.21
4C	Te	10^{17}	5.47	6.26	0.18
20C	Te	10^{17}	7.29	8.83	0.21
32C	Al	10^{17}	5.04	6.67	0.15
30C	Al	10^{17}	6.26	8.65	No data
27C	Al	10^{17}	11.6	12.89	No data
19C	Cl	10^{17}	1.25	1.46	No data
21C	Cl	10^{17}	1.16	1.46	0.17
22C	Cl	10^{17}	4.85	6.4	0.14
3C	Cu	10^{17}	0.25	0.27	0.27

CONCLUSIONS

Single-crystal samples doped with Te and Al showed a marked increase (~×10) in I_d and I_L values over earlier reported results on similarly doped polycrystalline samples. Doping with Al resulted in the maximum values of I_d and I_L, while the highest activation energy for conduction (lowest currents) was found in the Cu-doped UO_2. Overall, doped single crystals of UO_2 were much more electrically conductive than the doped polycrystalline UO_2. Doped single-crystal and polycrystalline UO_2 exhibited similar time-dependent behavior. The superlinear (i.e., nonohmic) voltage dependence of the measured currents and its time- and light-dependent changes were much slower than conventional material photoconductivity phenomena. Current sometimes changed in little steps, resembling a "switching" behavior (7). These steps appear to be unique to UO_2 and have now been confirmed for many doped single-crystal and polycrystalline samples.

Additional effort will be required to understand the details of the electrical conduction mechanisms in UO_2. We have initiated optical investigations that show a very shallow absorption edge that makes it difficult to define a bandgap. Earlier studies (5) suggested the possibility that the conductivity of UO_2 arises from ionic transport. However, because we have observed essentially single activated behavior down to ~150 K, we believe that this hypothesis is not likely. Another earlier interpretation (8) of the conductivity mechanism seems more appealing. In the later explanation, carriers are activated into a single band (a valence band because the samples are p-type). Such activation could arise from the *de facto* excitation of localized carriers into a state in which they are more mobile, in essence resulting in an activation of carrier mobility rather than carrier densities.

ACKNOWLEDGEMENTS

We acknowledge the cooperation of the National Renewable Energy (NREL) in permitting electrical and optical measurements of urania at its facilities. Our thanks extend to NREL's Electronic Devices and Materials Division, and especially the Amorphous Silicon Team, whose facilities and assistance we used to carry out the measurements. Jodi Donley of NREL's safety group provided efficient support in obtaining the permits required to characterize these samples at NREL.

This work was sponsored, in part, by the U.S. Department of Energy (EM-30) Depleted Uranium Uses Research and Development Project.

REFERENCES

1. R. R. PRICE, M. J. HAIRE, and A. G. CROFF, "Depleted Uranium Uses R&D Program," Waste Management 2001 Symposium, Tucson, Arizona, February 25–March 1, 2001.

2. T. T. MEEK et al., "Ion Implantation of UO_2," The Society for the Advancement of Materials and Process Engineering (SAMPE) 2002 Symposium and Exhibition, Long Beach, California, May 12-16, 2002, pp.1703-1710.

3. M. J. HAIRE, T. T. MEEK, and B. G. von ROEDERN, "Photoconductive Properties of Doped UO_2," The American Nuclear Society Winter Meeting, November 17–21, 2002, Washington, D.C.

4. B. B. von ROEDERN, T. T. MEEK, and M. J. HAIRE, "Some Electrical Properties of Ion-Implanted Urania—Part II," The Society for the Advancement of Materials and Process Engineering (SAMPE) 2003, Long Beach, California, May 11–15, 2003.

5. J. L. BATES et al., "Electrical Conductivity of UO_2: Part 1, Single Crystals," Battelle-Northwest (1986).

6. J. C. KILLEEN, "Effect of Niobium Oxide Additions on the Electrical Conductivity of UO_2," J. Nucl. Mater. **88**, 185–192 (1980).

7. S. R. OVSHINSKY, "Localized States in Gap of Amorphous-Semiconductors," Phys. Rev. Lett **36**, 1469 (1976).

8. S. ARONSON, J. E. RULLI, and B. E. SCHANERE, "Electrical Properties of Nonstoichiometric Uranium Dioxide," J. Chem Phys. **35**, 1382–88 (1961).

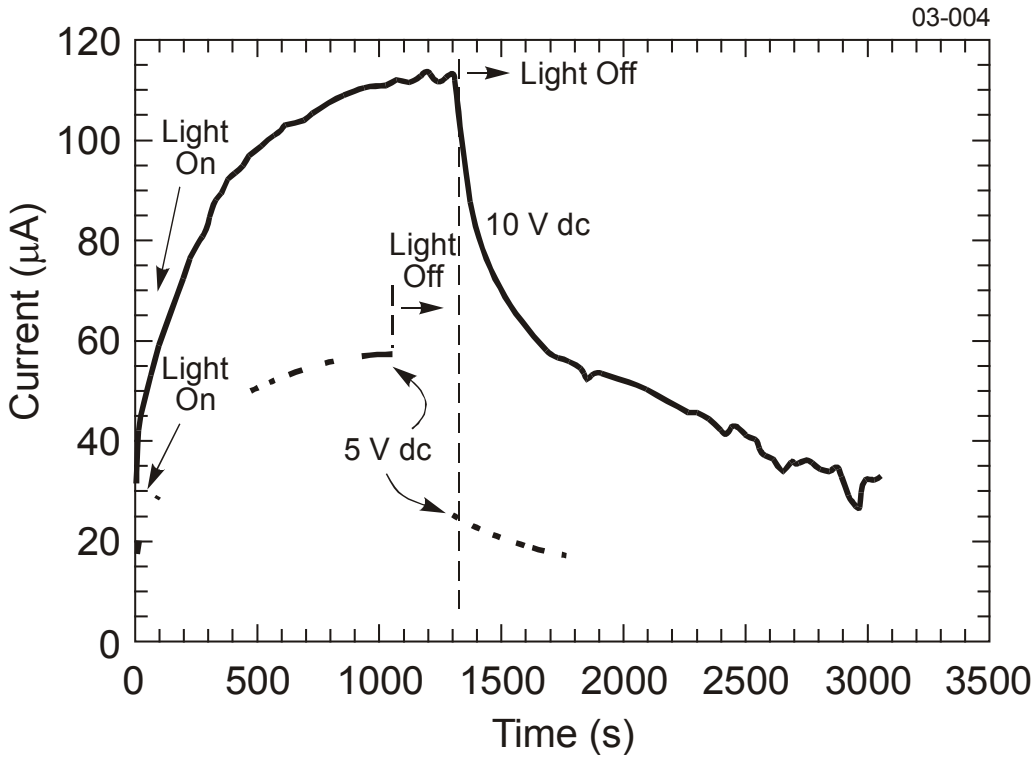

Fig. 1. Dark and light current versus time for intrinsic UO_2.

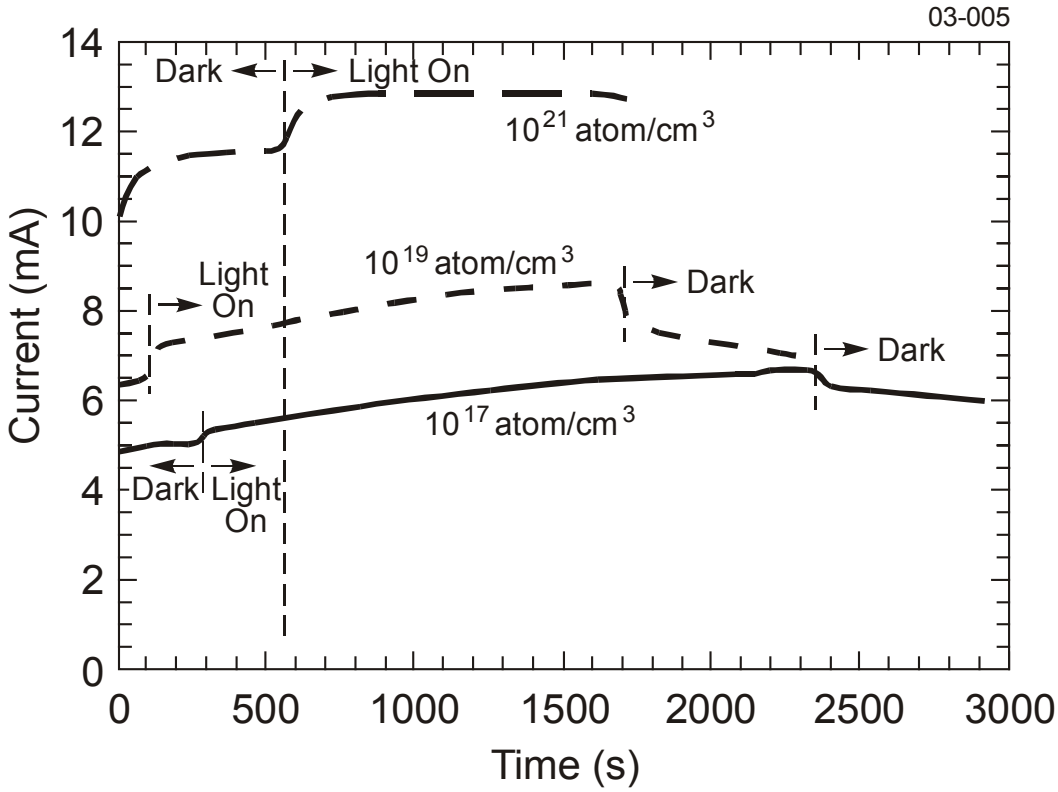

Fig. 2. Dark and light current versus time for Al-doped UO_2.

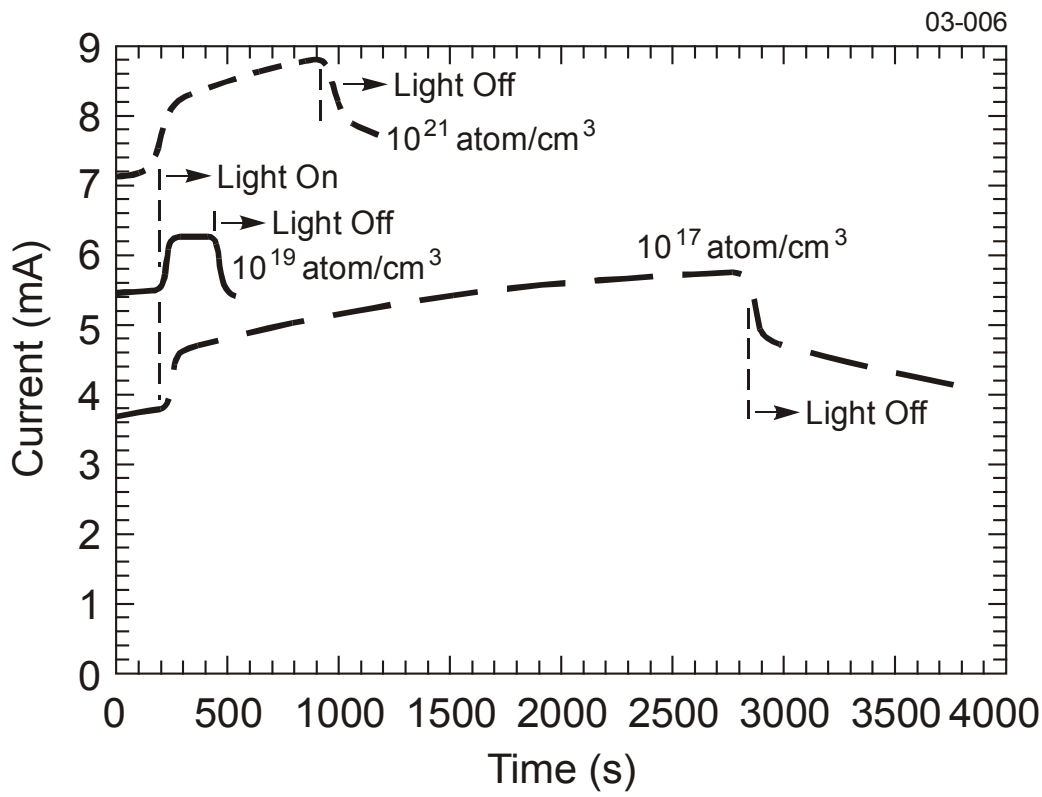

Fig. 3. Dark and light current versus time for Te-doped UO_2.

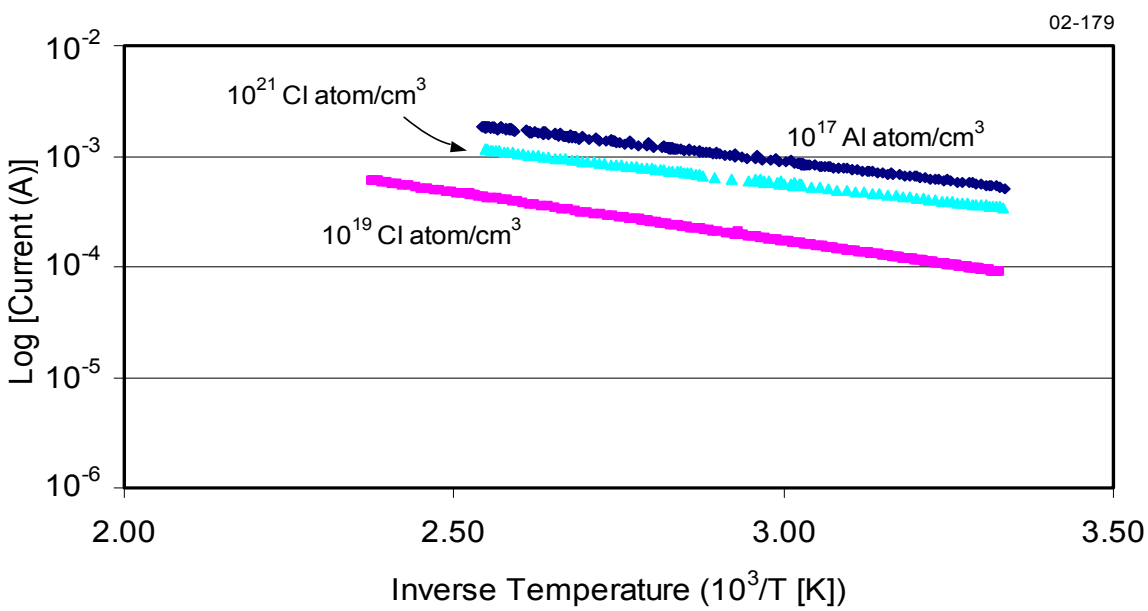

Fig. 4. Activated dark currents for one Al-doped and two Cl-doped UO_2 samples.